

Research Article

A Digital Health Monitoring Device Combining Sensing of Blood Pressure, Blood Sugar and Temperature

Divine Edem Junior Adjabeng, Mathias Vormawor, Benjamin Kommey*, Daniel Opoku, Nathaniel Ato-Sam

College of Engineering, Kwame Nkrumah University of Science and Technology, Kumasi, Ghana

*bkommey.coe@knust.edu.gh

Abstract

Access to affordable and portable multipurpose diagnostic devices remain a major challenge in developing parts of the world. These challenges affect the early detection and management of chronic diseases like hypertension and diabetes. This study focuses on the development of “Dygnox”, a multipurpose medical device that combines the functionalities of a thermometer, sphygmomanometer, and glucometer. An Arduino-based embedded control unit performs all signal conditioning, analog-to-digital conversion, and algorithmic computations needed for diagnosing while a LCD is used to display final measurements. Signal processing techniques including thermistor linearization, oscillometric envelope detection, glucose current detection through transimpedance conversion were implemented to convert raw data from the sensors into meaningful information. A proof-of-concept prototype was fabricated using a custom-etched printed circuit board and enclosed in a durable Polyvinyl Chloride casing. Via a thorough hardware and software testing, the signal conversion accuracy and the capability of the device to deliver clinically relevant readings in all the three diagnostic functions were confirmed.

Keywords: Health Monitoring Systems; Arduino; Multi-parameter Diagnostics; Embedded Systems; Biomedical Instrumentation; NTC Thermistor Calibration; Enzymatic Glucose Sensing.

INTRODUCTION

Disease monitoring and management are critical in healthcare centers and institutions. Unfortunately, current diagnostic tools provide some challenges such as the difficulty in device administration, high cost, and inconsistent data integration [1]. To confronts these challenges, In Ghana, the Ghana Health Services is providing affordable diagnostic equipment to clinics and chip compounds in rural areas [2]. There is therefore the need to minimize these challenges to avoid the impediment of early disease detection and medical treatment, especially for chronic disorders such as diabetes, fever, hypertension, and hypotension. Traditionally, health monitoring systems operate independently, demanding the use of different and individual sensors to monitor blood sugar levels, blood pressure, and temperature.

This work proposes a solution to solve these inefficiencies by creating a multifunctional diagnostic device that has a thermometer, glucometer, and sphygmomanometer integrated into one complete device. The proposed device, codename “*Dygnox*” is intended to digitize diagnostic operations and give a user-friendly interface. The development of this device aligns with Sustainable development Goal SDG 3, which focuses on ensuring healthy lives for people at all ages, as well as SDG 9, which focuses on innovation and infrastructure in health-care sector [3].

RELATED WORKS

Current research shows various improvements as well as some downsides in the three areas of focus. Reviewing papers in temperature sensing suggest thermal monitoring remains one of the most basic health checks used in the health sector; however, it faces measurement accuracy as it is frequently influenced by ambient environmental conditions. Kukharchuk *et al.* used Arduino-based systems to demonstrate that the application of STEM-based learning approaches for the calibration of NTC thermistors can improve measurement accuracy and consistency [4]. Although non-contact temperature measurement techniques such as surface plasmon resonance (SPR) enable rapid and highly sensitive temperature detection, their implementation is expensive and complicated making simple contact-based thermistors a more practical approach for low-cost point-of-care medical devices [5, 6].

Research in blood pressure monitoring describes the transition from mercury sphygmomanometers to digital oscillometric devices as an improvement to the usability and safety in blood pressure monitoring. This transition also introduces issues such as calibration errors and measurement differences between similar devices [7]. Reviews of emerging wearable and cuffless blood pressure monitoring technologies are being developed for continuous monitoring but many of these systems do not yet achieve the accuracy standards of conventional cuff-based devices [8]. Blood pressure readings can be affected by cuff positioning leading to some deviations in sequentially recorded values. Other Evaluations obtained from guided experiments have shown that systolic blood pressure readings can vary by several millimeters of mercury depending on whether measurements are taken at the upper arm or near the elbow [9, 10]. Moreover, digital sphygmomanometers that use microcontrollers and LED bar display have shown reduced measurement error under controlled testing conditions. This provides a mercury-free alternative for clinical environments [11]. Similarly, In the area of Glucose monitoring technologies there have been a transition from invasive laboratory-based testing toward self-monitoring blood glucose systems and wearable sensor platforms. Enzyme-based electrochemical sensing remains the most widely used approach because it is very reliable, and is suitability for portable applications [12]. To evaluate the importance of glucose measurement accuracy in the health sector, Clarke *et al.* introduced Error Grid Analysis (EGA), a method that evaluates glucose measurements based on how they affect medical decisions rather than just numerical accuracy [13]. Non-invasive laser-based glucose

sensing methods are being studied and offer painless testing, these systems however continue to face challenges related to accuracy and consistency when compared to established enzymatic strip-based methods, especially in low-resource settings [14].

MATERIALS AND METHODS

Figure 1 depicts the V-model implementation of the development methodology. The development process followed a simplified V-model. Details process descriptions are left out in order not to float the manuscript and thereby exceeding the required journal page limit. The left side of the model focused on concept definition and solution design, while the right side validated the feasibility of the concept. After defining the problem, the concept requirement defined the minimal functional capabilities needed to demonstrate the feasibility of the proposed solution to the problem. Major components and their interactions were identified under the high-level design and was detailed in the prototype design stage.

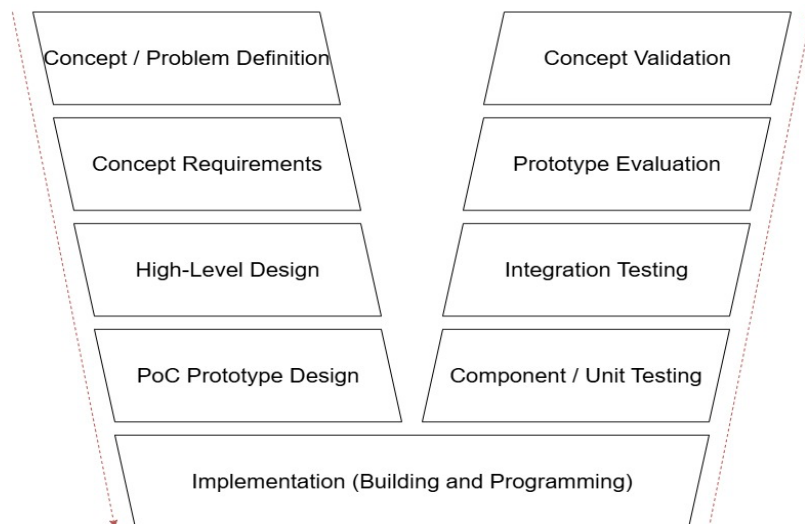


Figure 1. A simplified V-model development approach for the prototyping.

A working throwaway prototype was developed, which passed the unit and integrated testing phases. Experimental validation was conducted and proved the feasibility of the concept. The V-model has been systematically followed throughout the development of the system hardware and software prototype. The software part of the system is intended for a separate future manuscript publication.

Dygnox System Architecture

As shown in Figure 2, the system architecture of this diagnostic device consists of three main parts: the Physical Diagnostic Unit (PDU), the Embedded Control Unit (ECU), and the User Visualization Interface (UVI). All sensors and other mechanical components are

housed in the Physical Diagnostic Unit (PDU) and this is responsible for health reading information collection.

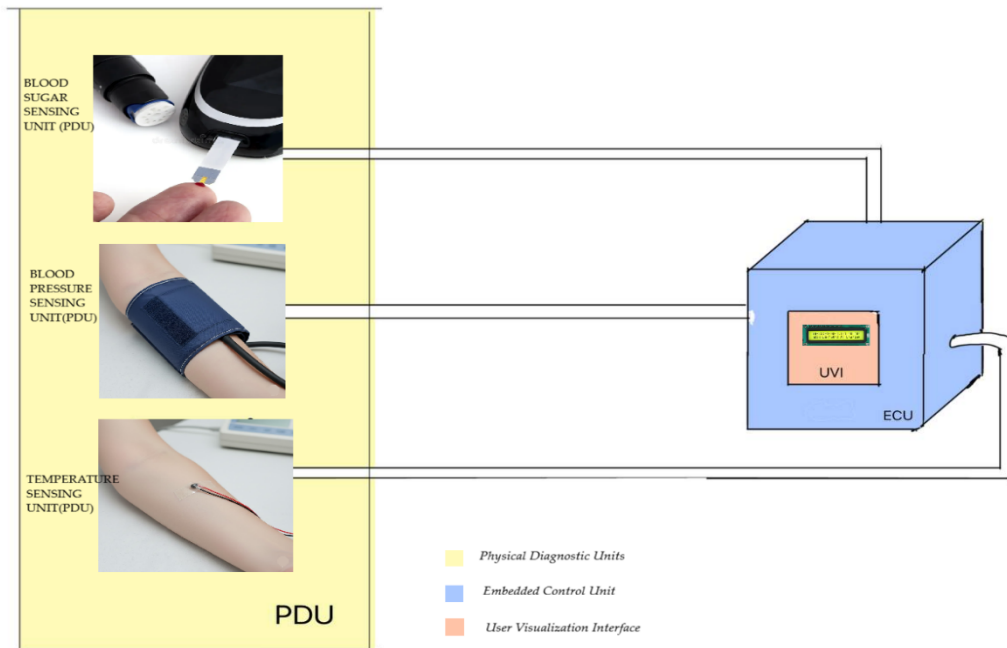


Figure 2. Dygnox System Architecture

In this case, the health readings are the body temperature, the blood pressure and the blood glucose or sugar levels. The user's physiological signals are read as inputs via sensors and later transmitted to the central processor, in this case the Embedded Control Unit (ECU) for further processing, analysis and evaluation. The ECU serves as the brain of the system and houses the microcontroller, in this case the Arduino. All data processing is done in the ECU. The ECU collects raw data via sensors and converts with the aid of the ADC these collected data into understandable values for the microcontroller via mathematical formulas. The timing of the air pumps as well as the release of valve which are used for the measurement of the blood pressure are all controlled and monitored through the embedded control unit (ECU).

As mechanical components require higher power than the sensors, the ECU is designed with a dual-power supply system to ensure that electronic signals remain stable, noise-free, and accurate. The UVI is the point of communication between the device and the user. The microcontroller sends the final, processed data to a 16x2 LCD screen to be displayed.

Dygnox Hardware Block Diagram

The hardware block diagram for Dygnox as shown in figure 3, illustrates the connection of the individual mechanical and electronic components that function together to achieve the diagnostic results. When the system is turned on by pushing the power button, the power from the battery source is regulated by a voltage regulator to prevent the microcontroller from receiving excessive power and to guarantee a consistent 5V reference for the sensors. To select a certain diagnostic function, the user interacts with the system

by pressing a button that toggles between operational modes for temperature, blood pressure, and blood sugar. Once a choice is selected, the preset calibration settings for that particular test are established.

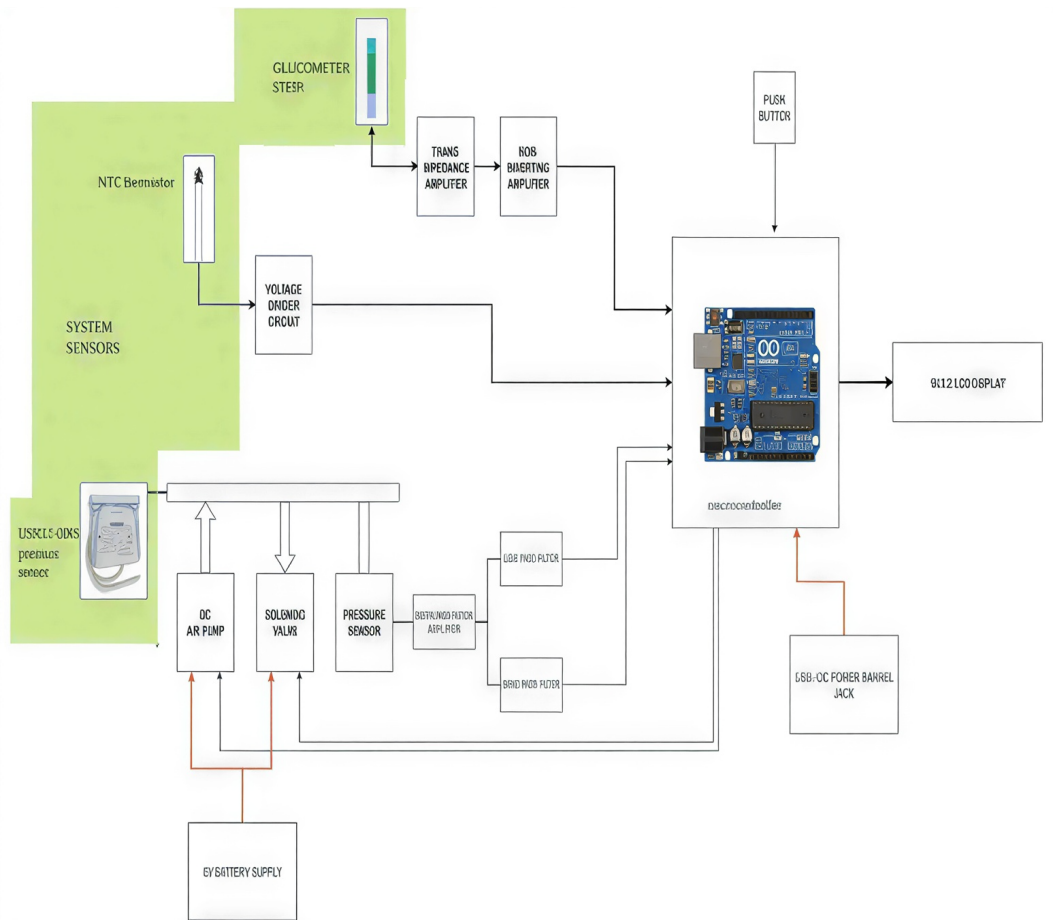


Figure 3. The complete block diagram for the diagnostic device.

The NTC thermistor and the US9111-006S pressure sensor of the device collect associated physical health data, while the glucometer interface collects electrochemical signals from the test strip. Sensor readings are sent to the microcontroller for processing. For blood pressure monitoring, the microcontroller uses the received data to perform logical operations, based on which it regulates the transistors and relays connected to the DC air pump, the solenoid valve, and the signal conditioning circuits, the electric air pump is also turned on to inflate the arm-cuff and is turned off once the target pressure is reached. The solenoid valve is then activated periodically to release air at a controlled rate, allowing the sensor to detect arterial pulses.

During blood sugar monitoring, a transimpedance amplifier converts the small current generated by the enzymatic reaction on the test strip into a voltage signal. This voltage is then digitized by an Analog-to-Digital Converter (ADC) and processed by the

microcontroller to determine the glucose concentration. For temperature monitoring, the NTC thermistor is used to detect body heat. These heat signals from the NTC thermistor pass through a voltage divider circuit to have the temperature-dependent resistance changed into a variable voltage. The analog signal is then sampled by the microcontroller's ADC. The microcontroller then reads the resulting voltage and applies a linearization formula to convert it into a precise temperature reading.

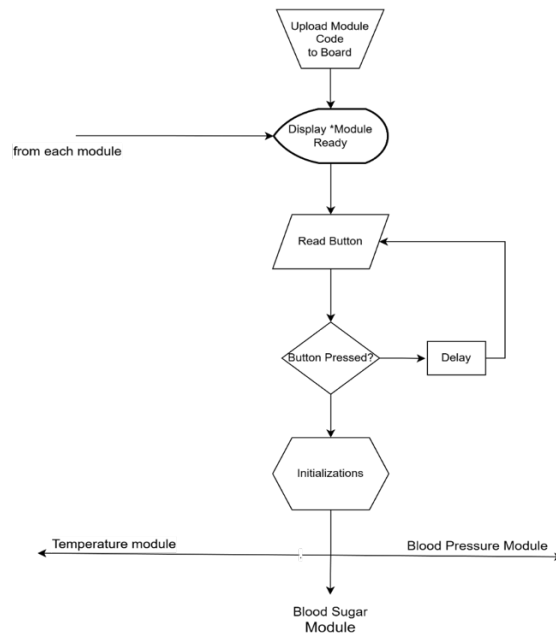
The data collected by the sensors, including temperature, blood pressure, and glucose levels, are then sent to the 16x2 LCD to be displayed to the user.

Dygnox system workflow

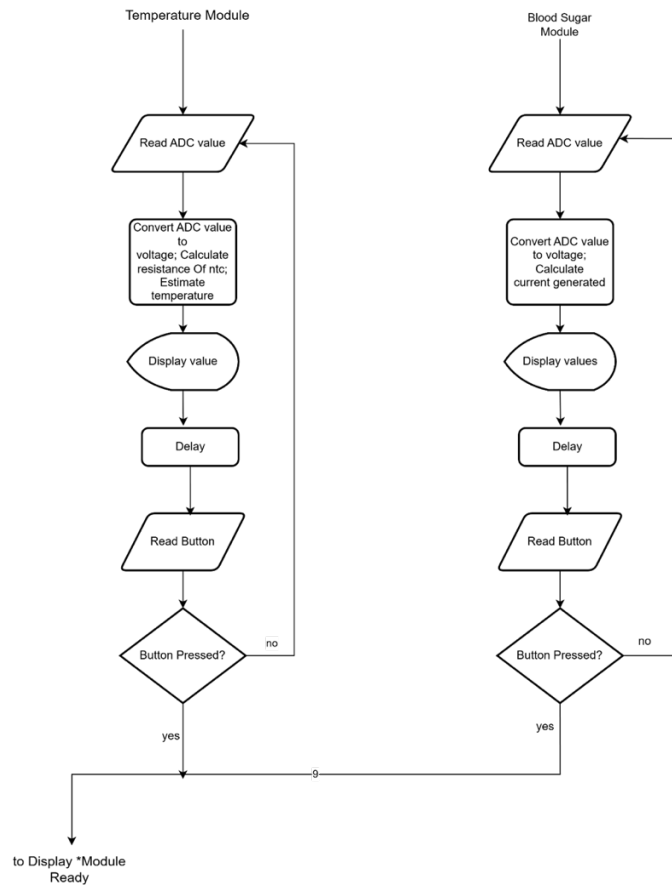
The Dygnox system workflow diagram as shown in Figure 4 (a), (b) and (c), depicts the logical sequence programmed into the microcontroller. After powering the system, the system undergoes an initialization phase where the I/O pins of the microcontroller are defined and the LCD is cleared for use. Thereafter, the system enters a waiting state, displaying a "ready" message while prompting the user to select a diagnostic mode. To select the desired diagnostic mode, the mode-selection push button must be pressed. The microcontroller continuously polls this input; each press, cycles the system through three preset states: Temperature, Blood Pressure, and Blood Sugar. Once a selection is made, the system executes the specific logic associated with that mode. If temperature mode is selected, the microcontroller reads the analog voltage from voltage divider circuit connected to the NTC thermistor and then performs a conversion to resistance and applies the linearization algorithm.

Then the result is displayed on the LCD. Selecting Blood Pressure Mode triggers the electric air pump to inflate the cuff to a preset threshold. Once reached, the microcontroller activates the solenoid valve to be pulsed slowly, bleeding the air allowing the US9111-006S sensor to capture the pressure oscillations. The microcontroller identifies the systolic and diastolic peaks and displays the results on the LCD. For Blood Sugar Mode, the system monitors the transimpedance amplifier for a signal from the glucose test strip. Upon detecting a signal, it calculates the glucose concentration based on the current created during enzymatic reaction on the test strip and outputs the result on the LCD.

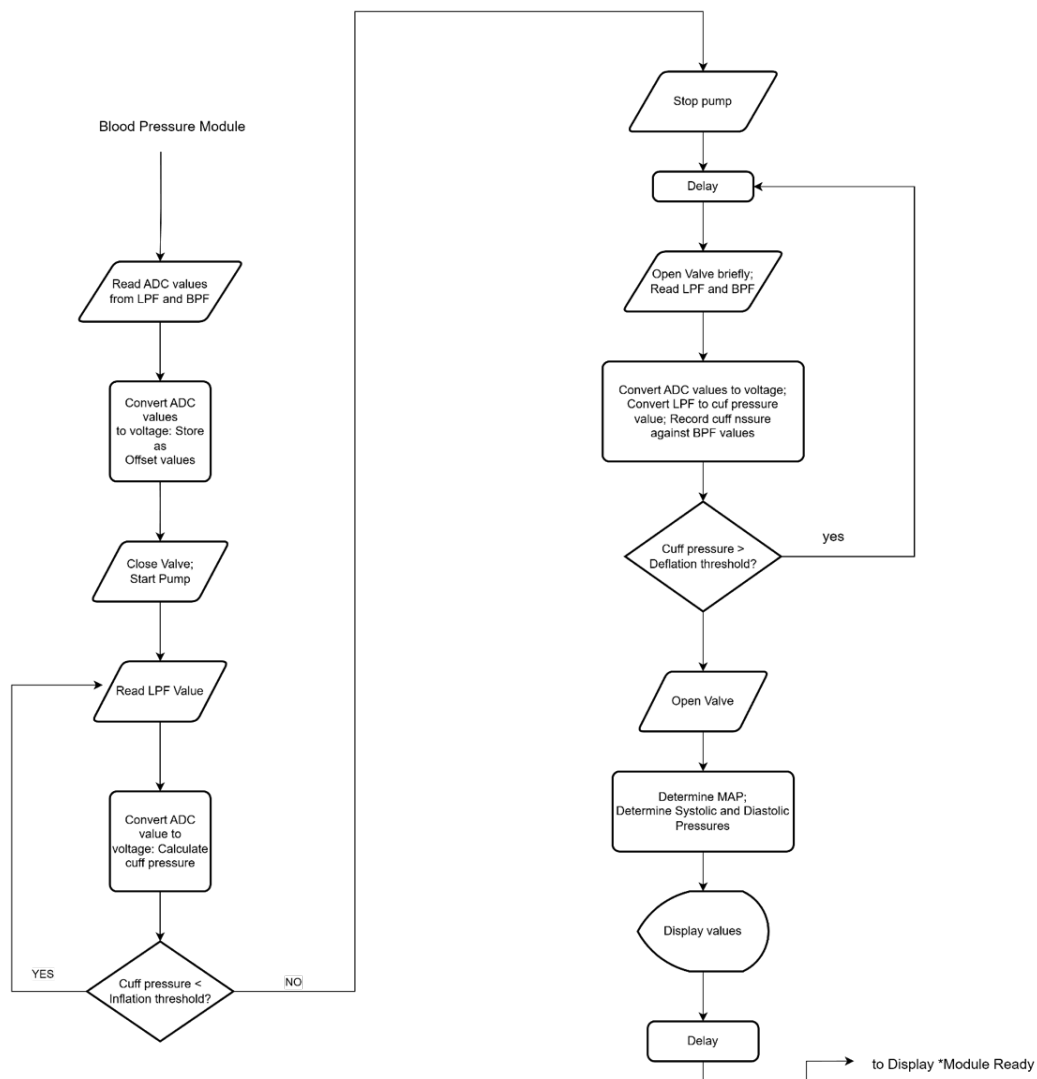
The system then returns to the initial mode-selection state after every results display; ready for the next operation.



(a)



(b)



(c)

Figure 4. Dygnox system workflow

Dygnox Signals Processing and Computational Logic.

The raw data acquired from the sensing modules are supplied as analog voltage signals, which require digitization and algorithmic transformation to produce clinically meaningful metrics.

Temperature Signal Linearization

The analog signal received by the controller is in the range of 0 - 1023 (10-bit resolution of the analog pins on the board) [15]. The temperature sensing module utilizes a voltage divider network. The sampled ADC value is first converted to the instantaneous voltage (V) across the thermistor using [16]

$$V = \left(\frac{\text{ADC}_{\text{value}}}{\text{ADC}_{\text{max}}} \right) \times V_{\text{supply}} \quad (1)$$

the thermistor resistance (R) was determined, using the following relationship

$$R = R_{\text{series}} \times \left(\frac{V}{V_{\text{supply}} - V} \right) \quad (2)$$

The absolute temperature (T_K) is derived using the Beta Model of the Steinhart-Hart equation, providing a linear output in Celsius (T_C) [17]

$$T_K = \left(\frac{1}{\frac{1}{T_{\text{nom}} + 273.15} + \frac{1}{\beta} \ln \frac{R}{R_{\text{nom}}}} \right) \quad (3)$$

$$T_C = T_K - 273.15$$

Glucose Computations

The system processes the output of the transimpedance amplifier for the blood glucose or sugar analysis, whereby generated current from the enzymatic reaction ($I_{\mu A}$) is calculated by analyzing the voltage drop across the feedback resistor (R_f) [18].

$$I_{\mu A} = \left(\frac{V}{R_f} \right) \times 10^6 \quad (4)$$

After which a comparison of the current against a pre-calibrated look-up table stored in the microcontroller's flash memory to estimate glucose concentration is performed.

Oscillometric Blood Pressure Extraction Processing

The method used in measuring the blood pressure in the work is the so-called oscillometric envelope detection. Here the sensor, in this case the pressure sensor is bifurcated into a low-pass filter for static cuff pressure and a band-pass filtered signals to extract the arterial oscillations

Given the following parameters, we derived the equation (5)

LPF is the Low-Pass Filter

$P(t)$ is the static cuff pressure and

BPF is the Band-Pass Filter

Static cuff pressure (in mmHg) is derived through linear mapping:

$$P = \max(0, V_{\text{LPF}} - V_{\text{offset,LPF}}) \times \left(\frac{P_{\text{FS}}}{V_{\text{FS}} - V_{\text{offset,LPF}}} \right) \quad (5)$$

where $P_{\text{FS}} = 300\text{mmHg}$ is the full-scale pressure and V_{FS} the full-scale voltage at that pressure.

To isolate the oscillometric envelope (E_n), the BPF signal is rectified and smoothed using an Exponential Moving Average (EMA) to filter out movement artifacts [19]:

$$E_n = (1 - \alpha)E_{n-1} + \alpha|V_{BPF} - V_{offset,BPF}| \quad (6)$$

where α is the smoothing factor ($0 < \alpha \leq 1$).

Let denote the maximum envelope amplitude, reached at cuff pressure $PMAP$:

The Mean Arterial Pressure $PMAP$ is identified at the peak amplitude of the envelope (E_{max}) [20].

$$E_{max} = \max_n E_n, \quad P_{MAP} = P(n_{peak}) \quad (7)$$

The systolic and diastolic pressures are then determined using fixed-ratio thresholding [20].

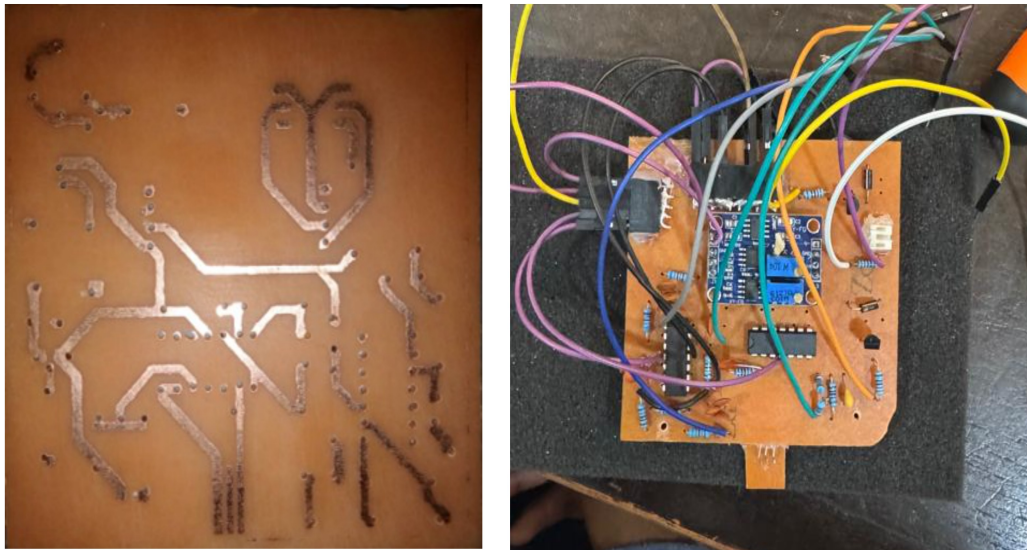
$$P_{SYS} = P(E \geq 0.5E_{max}, n \leq n_{peak}) \quad (8)$$

$$P_{DIA} = P(E \leq 0.7E_{max}, n \geq n_{peak}) \quad (9)$$

Dygnox system prototype design

The Dygnox system was designed using a custom-made Printed Circuit Board (PCB) to reduce errors that occur inevitably in manual wiring. The schematic diagram designed was converted into a physical circuit by using a special etching process; this process involved cutting a copper-clad laminate to the dimensions of the schematic using a cutting saw. Prior to that, the digital schematic is first mirrored and printed to ensure that the trace orientation aligns with the positions of the components upon transfer. This layout is then moved onto the copper-clad board by firmly attaching the paper onto the board and pouring a precise mixture of Acetone and Isopropyl Alcohol onto the combined unit after which a mechanical roller is pressed onto the unit to fuse the lines of the schematic to the copper surface.

Upon successful transfer of the schematic traces, the unit is submerged in a chemical etchant solution, typically Ferric Chloride ($FeCl_3$), to remove the unprotected copper while the sections covered by the toner remain intact. The board is cleaned using acetone to remove the remaining toner while revealing the copper signal paths underneath. Once the copper traces are exposed, the board is evaluated by checking for open-circuits or short-circuits that occur inevitably during the etching phase. Following the etching process, the board was dried, and then drilled for component mounting. The integration of components was performed through manual soldering, see Figure 5.



(a)

(b)

Figure 5. (a) Etched copper board (b) Manual components soldering.

The casing for the device as shown in Figure 6 was created using Polyvinyl Chloride (PVC). PVC was chosen for its high strength-to-weight ratio, availability as well as its dielectric properties [21]. The casing was designed not only to protect the electronics but also to provide a more familiar build suitable for clinical and domestic settings.

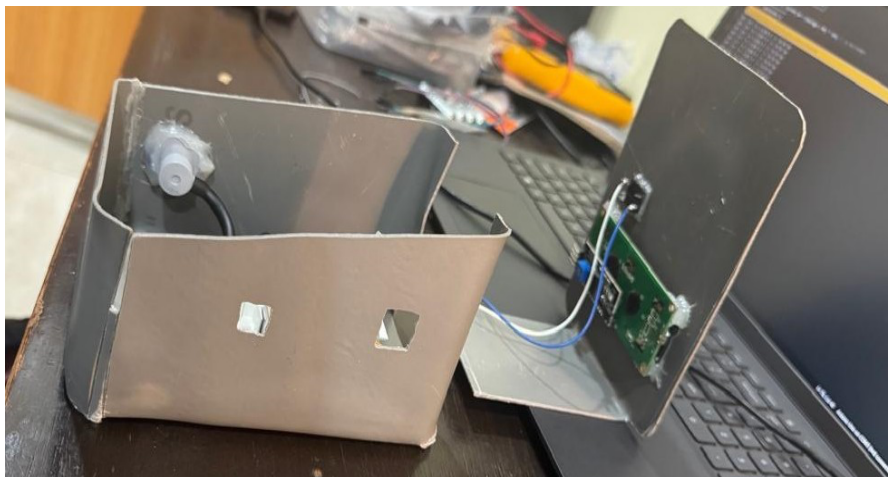


Figure 6. Molded PVC pipe for the casing of the prototype.

The final design phase as illustrated by figure 7. involved combining the populated PCB made from the etching technique with the Arduino development board and securing all mechanical and electronic components within the PVC housing. This ensures that the internal electronics are safeguarded from physical impact.

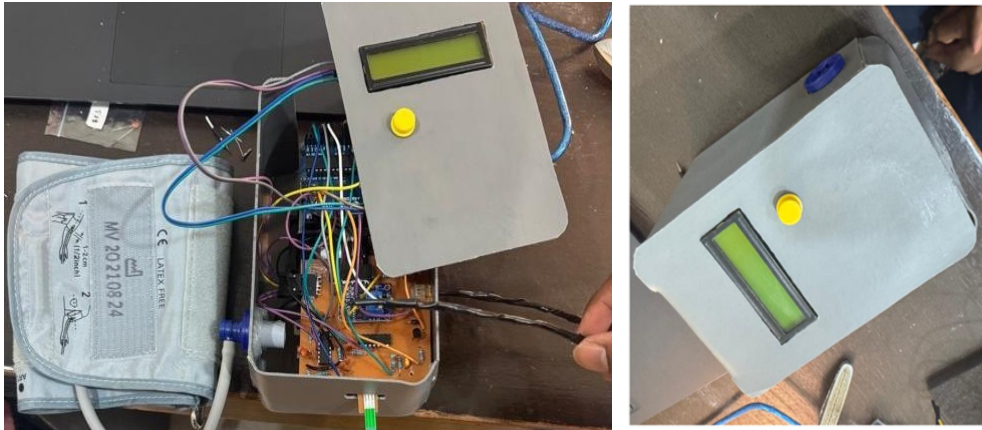


Figure 7. Population of the components into the PVC housing.

Dygnox System Software Design

Software used for Dygnox was written in C++ code in an Arduino Integrated Development Environment (IDE) and uploaded as sketches to the Arduino boards microcontroller. The C++ code is made up of methods and functions written for all the microcontroller's operations necessary for the proper functioning of Dygnox.

The operational sequence the code is made up of follows the sequence illustrated in the system flowchart mentioned in Figure 3. Other Key functions of the code include a debounce algorithm for the mode-selection button, an auto-calibration routine for the pressure sensor at startup, as well as an EEPROM-write cycle to ensure there is persistence data after a measurement.

TESTING AND EVALUATION

Hardware Testing

The hardware components of Dygnox underwent a rigorous testing process. This was to ensure accuracy in the performance of these components. The analog signal conditioning circuits, specifically the amplifiers and active filters, were modeled and simulated using LTspice. This enabled an evaluation of the frequency response and gain settings of those signal conditioning circuits. The evaluation confirmed that the band-pass filters were properly tuned to the 1-5 Hz range required for arterial oscillation detection needed for blood pressure monitoring.

To confirm that the sensors and actuators modules functioned as expected, each module was tested independently. As shown in Figure 8(a), a function generator and a digital storage oscilloscope were used to tune the gain and DC offset of the amplifier ensuring that the low-frequency arterial oscillations passed by the band-pass filters remained within the dynamic range of the microcontroller's 10-bit ADC without clipping. Simultaneously, figure 8(b) shows that the temperature module was calibrated using a digital multimeter

The monitor showed consistent voltage and resistance conversions for the temperature module, which resulted in a stable reading of 23.70°C. On the other hand, the blood sugar (TIA) test showed that when a test strip was inserted, the system detected current in microamps produced during the enzymatic reaction. Additionally, the blood pressure logs that were captured showed the transition from cuff inflation to cuff deflation, recording the pressure drops and oscillation amplitudes right until the final systolic and diastolic values were calculated.

System Comparative Analysis

To clearly Demonstrate the advantages this proof-of-concept device has over the equivalent standalone devices sold commercially, a comparative analysis was performed through guided research to compare both instances. A market survey of some selected products was conducted using Amazon.com as it is a standardized international store to determine the average retail cost of individual diagnostic units [22]. The cost estimation for the system prototype are shown in Tables 1 and 2. Since this is a prototype cost estimation, the end product cost may vary slightly from what has given here, yet still the aim of making the whole system cost effective is achievable. A comparative cost analysis of the designed system prototype is shown in Table 2 with some selected standalone devices.

Table 1. Prototype Cost Estimation in US Dollars

System Prototype	Estimated Cost
PVC case	1
Arduino Board	10
Cuff	6
Thermometer probe	5
Test strip generic	5
Other sensors	6
Misc.	10
Total	43

Table 2. Comparative Cost Analysis in US Dollars

System Prototype	Blood Pressure	Blood Sugar	Temperature	Total Cost
23	Omron (37.69)	On-call (9.99)	FDK (19.99)	67.67
23	Sinocare (16.99)	VivaGuard (26.99)	Safety (9.84)	53.82
23	Alcedo (28.45)	Contour (34.85)	Classic (22.49)	85.79

System Cost Estimate Discussions.

Analysis from the tables 1 and 2 demonstrates a significant reduction in cost expressed in percentage based on equation (10).

$$\text{cost reduction} = \left(\frac{\text{total cost of separate devices} - \text{Dygnox cost}}{\text{total cost of separate devices}} \right) \times 100 \quad (10)$$

From the calculations, a cost reduction of about 40 percent is achievable.

It was observed that beyond the reduction in weight and components, there are other financial usability advantages. Whilst the standalone devices require their individual common components such as the microcontroller, the display unit and power regulation circuits, the integrated device uses just one for all. The single unit designed prototype eliminates the need for multiple supporting electronics, sensors and other controls and thereby reducing the overall hardware performance and costs which also leads to improvement in manufacturing efficiency. Another advantage is that the single device can be assembled with only one printed circuit board (PCB) and common case or enclosure instead of producing separate and individual device components. A PVC enclosure was used for the prototype, making it very cost-effective. Worth mentioning is also the power source sharing of the designed system prototype. This single source approach, require fewer batteries and thereby contributing to lower cost and maintenance requirement, which in the long-term, particularly in rural clinics and chip compounds where resource and tools maintenance are very limited, could lead to notable operational cost savings.

System Energy Consumption

Table 3 contains the power consumption comparison between some selected standalone devices and proof-of-concept prototype.

Table 3. Comparative Energy Consumption Analysis

Device	Operating Voltage	Active Current	Power Consumption
Blood Pressure Monitor	6V	600mA	3.6W
Blood Sugar Monitor	3V	3mA	0.036W
Digital Thermometer	1.5-9V	4mA	9mW
Total consumption		607mA	3.65W
Prototype system	5V	250mA	1.85W

Having all three diagnostic modules draw from one power delivery one after the other provides a rather strategic reduction in power, though this also requires that this power delivery is a more robust one than the ones in the single stand-alone devices. To further explain this strategic reduction in power each of the separate devices will bring about three separate voltage regulators, filtering components, and power conversion stages. As a result, these three independent systems will bring about repeated power losses caused by conversion inefficiencies and parasitic current consumption such as quiescent current

draw. Additionally, In the designed prototype, a single 16×2 LCD display is powered to display information for all three diagnostic operations. In contrast, the three standalone devices would require powering separate displays, backlight drivers, and display microcontrollers to produce the same outcome.

The results show that the combined power consumption of the three separate standalone diagnostic devices could be approximately 3W during active operation. This is in comparison to the integrated prototype system producing a consumption outcome of about 0.325 W during monitoring conditions excluding blood pressure monitoring, with a temporary peak of approximately 1.825 W during blood pressure monitoring due to the pneumatic pump usage.

Taking the average power of the three stand-alone devices to be ≈ 3 W. And the power of designed prototype to be ≈ 0.325 W during normal operations then the percentage reduction is expressed via equation (11).

$$\text{Power Reduction (\%)} = \left(\frac{\text{Standalone Power} - \text{Dygnox Power}}{\text{Standalone Power}} \right) \times 100. \quad (11)$$

Resulting in over 70% reduction during operations without BP measurements. Further calculations from the table shows that even during blood pressure measurements where the designed prototype power rises to 1.825W, the system still achieves over 30% reduction in energy consumption.

Physical Portability and Volume Reduction.

The three separate diagnostic devices will occupy more space and hence hinder the ease of portability of a single device. Each device requires its own plastic enclosure, internal mounting structure, and supporting mechanical components. As a result, when multiple diagnostic tools are required for clinical assessment, the total physical volume increases due to the presence of multiple housings as well as multiple electrical components. In contrast, the prototype system integrates the thermometer, glucometer, and blood pressure monitoring circuits into a single PVC enclosure reducing the volume it occupies

The device volume of each device can be calculated as;

$$\text{Volume} = \text{length} \times \text{Width} \times \text{Height}. \quad (12)$$

For the designed prototype, all diagnostic circuits are housed within a single enclosure, resulting in a significantly reduced total system volume.

The table 4 highlights the dimensions and some estimations. The results from the table, it is clear that integrating all three devices would significantly reduce both system volume and overall device weight, which directly would improve portability and thereby aiding in cases where healthcare workers often need to transport diagnostic equipment between multiple communities.

Table 4. Other Comparative Analysis

Device	Length (cm)	Width (cm)	Height (cm)	Volume (cm)
Blood Pressure Monitor	16	11	7	1232
Blood Sugar Monitor	10	5	2	100
Digital Thermometer	14	2	2	56
Total estimated volume		607mA	3.65W	1388
Prototype system	n.a-	n.a-	n.a-	n.a

System Complexity and Reliability.

Standalone diagnostic devices typically have their dedicated user control interfaces, each with its own button layout and operating procedure. This implies that healthcare workers learn to use these different user control interfaces when performing each diagnostic operation. The designed system simplifies all of it by providing a unified user interface through which all diagnostic operations are accessed. The system prototype operation is intentionally simplified through a minimal user control interface consisting of two primary buttons: one button is used to power the system on, while a second button allows the user to switch between the available monitoring modes, these are temperature, blood pressure, and glucose measurement.

CONCLUSION

In conclusion, this study proved the capabilities of the integration of multiple diagnostic modules into a single device. The user-friendly prototype was able to overcome the challenges of cost, accessibility, and usability. It also provided precise readings on the measurements of temperature, blood sugar levels, and blood pressure. The device is able to minimize the use of individual devices, hence reducing the electronic waste and energy consumption associated with those individual devices. The significance of this project lies in the fact that it demonstrates the potential of embedded systems and biomedical engineering in transforming the field of healthcare delivery systems. With further refinement, the potential of the designed prototype codenamed Dygnox is immense in the field of preventive healthcare, the management of chronic diseases, and the global initiative towards an affordable and accessible medical solutions.

The key findings of this work is that beyond the reduction in weight and components, there are other financial usability advantages. Whilst the standalone devices require their individual common components such as the microcontroller, the display unit and power regulation circuits, the integrated device uses just one for all. The single unit designed prototype eliminates the need for multiple supporting electronics, sensors and other controls and thereby reducing the overall hardware performance and costs which also leads to improvement in manufacturing efficiency and reduction in environmental

pollutions. Another advantage is that the single device can be assembled with only one printed circuit board (PCB) and common case or enclosure instead of producing separate and individual device components. A PVC enclosure was used for the prototype, making it very cost-effective. Worth mentioning is also the power source sharing of the designed system prototype.

CONFLICT OF INTERESTS

The authors confirm that there is no conflict of interest associated with this work and publication.

REFERENCES

1. Mumtaz, H., Riaz, M. H., Wajid, H., Saqib, M., Zeeshan, M. H., Khan, S. E., Chauhan, Y. R., Sohail, H., Vohra, L. I., Current Challenges and Potential Solutions to the Use of Digital Health Technologies in Evidence Generation: A Narrative Review. *Front. Digit. Health* **2023**, *5*, 1203945.
2. Ministry of Health, *National Healthcare Quality Strategy (Revised Edition) 2024–2030*, Republic of Ghana, **2024**, pp. 1–68.
3. United Nations, The 17 Goals | Sustainable Development. Available from <https://sdgs.un.org/goals> (accessed date 11 January 2026).
4. Kukharchuk, R., Vakaliuk, T., Zaika, O., Riabko, A., Medvediev, M., Implementation of STEM Learning Technology in the Process of Calibrating an NTC Thermistor and Developing an Electronic Thermometer Based on It. *CTE Workshop Proc.* **2023**, *10*, 251–264.
5. Garcia-Ortiz, C.E., Peña-Gomar, M., López, R., Galaviz-Mosqueda, A., Coello, V., Fixed-Angle Surface Plasmon Resonance Thermometer for Accurate Temperature Monitoring. *Microw. Opt. Technol. Lett.* **2025**, *67*(1), e70070.
6. Okpaga, D.M., Agbo, P., Design, Construction and Calibration of a Multi-Scale Digital Thermometer. *IOSR J. Eng.* **2022**, *12*, 7–14.
7. Mousavi, S.S.; Reyna, M.A.; Clifford, G.D.; Sameni, R. A Survey on Blood Pressure Measurement Technologies: Addressing Potential Sources of Bias. *Sensors* **2024**, *24*, 1730.
8. Kumar, S., Yadav, S., Kumar, A., Blood Pressure Measurement Techniques, Standards, Technologies, and the Latest Futuristic Wearable Cuffless Know-how. *Sens. Diagn.* **2024**, *3*, 181–202.
9. Zhu, X. Y., Zhang, P. H., Huang, W. Y., Huang, W., Tang, X. H., Yu, H., Wang, S. N., The Impact of Sphygmomanometer Placement and Cuff Placement on Blood Pressure Measurements. *Front. Cardiovasc. Med.* **2024**, *11*, 1388313.
10. Hodgkinson, J., Lee, M. M., Milner, S., Bradburn, P., Stevens, R., Hobbs, F., Koshiaris, C., Grant, S., Mant, J., McManus, R., Accuracy of Blood-Pressure Monitors Owned by Patients with Hypertension (ACCURATE Study): A Cross-Sectional, Observational Study in Central England. *Br. J. Gen. Pract.* **2020**, *70*, bjgp20X710381.
11. Irianto, B., Sumber, S., Haq, E., Asghari, M., Sphygmomanometer with LED Bar Display to Improve the Blood Pressure Reading Accuracy. *J. Teknokes* **2022**, *15*, 154–160.

12. Lee, H., Hong, Y. J., Baik, S., Hyeon, T., Kim, D.H., Enzyme-Based Glucose Sensor: From Invasive to Wearable Device. *Adv. Healthcare Mater.* **2018**, 7(8), 1701150.
13. Clarke, W.L., Cox, D., Gonder-Frederick, L. A., Carter, W., Pohl, S. L., Evaluating Clinical Accuracy of Systems for Self-Monitoring of Blood Glucose. *Diabetes Care* **1987**, 10(5), 622–628.
14. Ibrahim, F., Mustafa, Z., Lateef Khudaraham, A., A Portable Noninvasive System for Detecting Blood Glucose Levels Using a Laser-Based Sensor. *Al-Nahrain J. Eng. Sci.* **2024**, 27, 19–24.
15. Arduino AG, *Arduino Uno Rev3*, Arduino AG, Italy, 2019, accessed May 19, **2025**.
16. Microchip Technology, *ATmega328P 8-Bit AVR Microcontroller with 32K Bytes In-System Programmable Flash Datasheet*. Available from <https://ww1.microchip.com/downloads/en/DeviceDoc/ATmega328P-Data-Sheet-40001906C.pdf> (Accessed date on 10 January 2026).
17. Steinhart, J. S., Hart, S. R., Calibration Curves for Thermistors. *Deep Sea Res. Oceanogr. Abstr.* **1968**, 15(4), 497–503.
18. Franco, S., *Design with Operational Amplifiers and Analog Integrated Circuits*, 4th ed., McGraw-Hill, New York, **2015**.
19. Drzewiecki, G., Hood, R., Apple, H., Theory of the Oscillometric Maximum and the Systolic and Diastolic Detection Ratios. *Ann. Biomed. Eng.* **1994**, 22(1), 88–96.
20. Lim, P.K., Ng, S.-C., Jassim, W.A., Redmond, S.J., Zilany, M., Avolio, A., Lim, E., Tan, M.P., Lovell, N.H. Improved Measurement of Blood Pressure by Extraction of Characteristic Features from the Cuff Oscillometric Waveform. *Sensors* **2015**, 15, 14142-14161.
21. Edo, G. I., Ndudi, W., Ali, A. B. M., et al., Poly(vinyl chloride) (PVC): An Updated Review of Its Properties, Polymerization, Modification, Recycling, and Applications. *J. Mater. Sci.* **2024**, 59, 21605–21648.
22. Amazon. Available from <http://amazon.com/> (Accessed date 5 January 2026).